

# Design and Analysis of Quantum Dot Laser diode for Communication Applications

Dr. Thaira Zakaria Al-Tayyar\*,  
and Jassim Mohammed Sahan\*\*

## ABSTRACT

Semiconductor laser diodes are important components in advanced optical fiber communication systems. Recent progress in nanostructure technology of quantum dot (QD), as active region, has led to the development of QD laser diodes which are superior to bulk, quantum-well or quantum wire laser diodes.

Design model of InAs QD laser diode structure is proposed in this paper; the proposed model of QD is disk shaped its height is 2 nm and diameter is 14 nm, surface density per layer is  $7 \times 10^{12} \text{ cm}^{-2}$ , number of QD layers are five, wetting layer thickness is 1nm and barrier thickness is 90 nm, the dimensions of the proposed model have an active region of length 800  $\mu\text{m}$ , width 12  $\mu\text{m}$ , and a height of 375 nm.

The evaluation of the proposed model is based on rate equations model. The results show that the QD laser diode has a lower threshold current 2.93 mA, threshold current density 30.42  $\text{A/cm}^2$ , bias voltage 0.97 V, while output optical power range is (0-25 mW) under wavelength range (1298-1305 nm). The model gain of the ground state is  $44.6 \text{ cm}^{-1}$ .

**Keywords:** Quantum dots, InAs, laser diode, rate equations.

---

\* *Electrical Engineering Department, University of Technology,*  
Email: [dr.tyra.uot@hotmail.com](mailto:dr.tyra.uot@hotmail.com)

\*\* *College engineering, Al-Nahrain University,*  
Email: [jasimsahan@gmail.com](mailto:jasimsahan@gmail.com)

## 1-INTRODUCTION

Semiconductor nano-particles, often referred as quantum dots (QDs), are semiconductor particles with physical dimensions smaller than the exciton Bohr radius (which is defined as the distance between the proton and electron in a hydrogen atom in its ground state (GS)) and are confined in three spatial directions [1]. Essentially, a semiconductor QD is a region of material a few nanometers in size where the carriers are confined. These carriers can be electrons, holes (missing electrons), or excitons (bound electron hole pairs).

The charge carriers are confined in a nanoscale box of one semiconducting material (in the case of the reported research, Indium Arsenide). That box or ring is surrounded by another semiconducting material GaAs (Gallium

Arsenide in the reported research) which presents a potential barrier to the motion of the carriers out of the box. Researchers call QDs as "artificial atoms", because the charge carriers in them behave the same way that orbiting electrons behave around the nucleus of an atom. In other words, the charge carriers in QDs can absorb or emit discrete amounts of energy as atoms do. [13]

The discovery of self-assembling of QDs opened a possibility of mass-production of QDs and gave an additional impact to their investigation. The self-assembling principle is based on the fact that during epitaxial by some growth conditions planar growth changes to 3D growth, forming objects with quantum confinement in all 3Ds. The InGaAs QDs on GaAs substrate open a possibility to obtain an emission wavelength over a very wide range from

0.95  $\mu\text{m}$  up to 1.55  $\mu\text{m}$ . Such long wavelengths could not be achieved using InGaAs quantum well due to the formation of misfit dislocations caused by a larger misfit strain [2].

In QDs carriers are three dimensions (3D) confined and the modification of electronic properties is quite stronger than quantum well and quantum wire. Also, in QDs, the energy levels are discrete and transitions between electrons and holes are comparable with transitions between discrete levels of single atoms. The QD lasers have demonstrated both theoretically and experimentally many properties, such as high optical gain, high-speed operation, ultra-low and temperature-stable threshold current density, broad modulation bandwidth, and narrow spectrum linewidth primarily due to the delta-function like density of states [3].

#### 2-Four-Level Rate Equations Model

As with any other semiconductor light source, also in QD lasers, there are the well-known electronic transitions between the conduction band (CB) and valence band (VB). The model can be divided into two parts, photon equations and electron equations. Thus, QD lasers are modeled with four carrier rate equations, two for GS, Excitation state (ES) and the latter is for wetting layer (WL) and separate confinement heterostructure (SCH) barrier layer with one rate equations related to photon populations. The presence of more than one state in the dot, is then, taken into account by including the ES.

The numerical model of the QD laser holds under the assumption that the active region consists of only one QD ensemble, where QDs are interconnected by WL. It has been assumed that each QD has only two confined energy states, the GS and the ES. The carrier energy levels are shown in Figure (1).

The carrier dynamics of the initial excitation position and energy level within

the barrier towards the QD-GS as follows [4],

- Carriers are injected in the SCH barrier at rate  $I/q$ , where  $I$  is the injection current,  $q$  is the elementary charge,
- Relax in the WL state at rate  $1/\tau_{c,sch}$  or escape back in the barrier at rate  $1/\tau_{e,wl}$ ,
- From the WL they can be captured in the dot. Therefore, the WL state acts as a common reservoir from which the carriers are captured in the ES at rate  $1/\tau_{c,wl}$  and from the ES to the GS at rate  $1/\tau_{c,ES}$  where, the times  $\tau_{c,sch}$ ,  $\tau_{c,wl}$  and  $\tau_{c,ES}$  are the average capture times from the SCH to the WL, from the WL to the ES and from the ES to the GS respectively,
- Carriers escape also from the GS back to the ES at rate  $1/\tau_{e,GS}$  or from the ES back to the WL at rate  $1/\tau_{e,ES}$  where the emission times  $\tau_{e,GS}$  and  $\tau_{e,ES}$  are the escape time from the GS back in the ES and the escape from the ES back into the WL,
- Carriers can also recombine with radiative and nonradiative processes from the SCH, the WL and the various confined states with rates  $1/\tau_{rs}$ ,  $1/\tau_{rw}$ ,  $1/\tau_r$  respectively.

The rate of photons emitted out of the cavity is  $S_p/\tau_p$ , with  $\tau_p$  the corresponding photon lifetime of the mode and  $S_p$  is the photon occupation probability. It is assumed that the stimulated emission can take place only due to recombination between the electron and hole in the GS. The diffusion, relaxation, recombination, and escape processes of carriers are shown in Figure (1) [4].

Since there are a small number of carriers in the QD, depending on the number of states, it is beneficial to represent the carrier rate equations in the dot by the rate equations of the occupation probability of the QD states. The resulting REs system for the carrier occupation probability is as follows [5],

$$\frac{dP_{sch}}{dt} = \frac{I}{e} - \frac{P_{sch}(1 - P_{wl})}{\tau_{c,sch}} + \frac{P_{wl}}{\tau_{e,wl}} - \frac{P_{sch}}{\tau_{sr}} \quad (1)$$

$$\frac{dP_{wl}}{dt} = \left( \frac{P_{sch}}{\tau_{c,sch}} + \frac{4P_{ES}}{\tau_{e,ES}} \right) (1 - P_{wl}) - \frac{P_{wl}}{\tau_{e,wl}} - \frac{P_{wl}}{\tau_{c,wl}} (1 - P_{ES}) - \frac{P_{wl}}{\tau_{wr}} \quad (2)$$

$$\frac{dP_{ES}}{dt} = \left( \frac{P_{wl}}{4\tau_{c,wl}} + \frac{P_{GS}}{2\tau_{e,GS}} \right) (1 - P_{ES}) - \frac{P_{ES}}{\tau_{e,ES}} (1 - P_{wl}) - \frac{P_{ES}}{\tau_{c,ES}} (1 - P_{GS}) - \frac{P_{ES}}{\tau_r} \quad (3)$$

$$\frac{dP_{GS}}{dt} = \frac{2P_{ES}(1 - P_{GS})}{\tau_{c,ES}} - \frac{P_{GS}(1 - P_{ES})}{\tau_{e,GS}} - \frac{P_{GS}}{\tau_r} - v_g \Gamma g_{GS} S_p \quad (4)$$

$$\frac{dS_p}{dt} = v_g \Gamma g_{GS} S_p - \frac{S_p}{\tau_p} + \beta \frac{2P_{GS}}{\tau_r} \quad (5)$$

where  $P_{ES}$  and  $P_{GS}$  are occupation probabilities of ES, and GS of a QD respectively and  $P_{wl}$ ,  $P_{sch}$  and  $S_p$  the WL and SCH population and the photon occupation respectively.

Occupation probabilities for GS and ES are defined as [6]

$$P_{GS} = \frac{n_{GS}}{2N_D} \quad (6)$$

$$P_{ES} = \frac{n_{ES}}{4N_D} \quad (7)$$

$$P_{wl} = \frac{n_{wl}}{N_D} \quad (8)$$

$$P_{sch} = \frac{n_{sch}}{N_D} \quad (9)$$

$$S_p = \frac{n_p}{N_D} \quad (10)$$

where,  $n_{GS}$  is the number of electrons in the GS,  $n_{ES}$  is the number of electrons in the ES,  $n_{sch}$  is the carrier number in the SCH,  $n_{wl}$  is the carrier number in the WL,  $n_p$  is the photon number,  $N_D$  is the total number of QDs,  $P_{wl}$  is the WL population,  $P_{sch}$  is the SCH population and  $S_p$  is the photon occupation.

The carrier escape times relate to the carrier capture times as follows [4],

$$\tau_{e,GS} = \tau_{c,ES} \frac{D_{GS}}{D_{ES}} e^{\frac{E_{ES}-E_{GS}}{K_B T}} \quad (11)$$

$$\tau_{e,ES} = \left( \frac{D_{ES} N_d}{\rho_{wl}} \right) \tau_{c,wl} e^{\frac{E_{wl}-E_{ES}}{K_B T}} \quad (12)$$

where, the  $D_{SG}$  and  $D_{ES}$  are the degeneracies of the GS and ES levels, respectively.

The  $E_{GS}$ ,  $E_{ES}$  and  $E_{wl}$  are the energies of the GS, ES and WL level, respectively, the  $K_B$  is the Boltzmann constant, and  $T$  is the degree of temperature in  $K^o$ . The carrier escape time from the ES depends on the ratio between the number of available states in the QDs and in the WL.

The escape time from the WL to the SCH is given by [7],

$$\tau_{e,wl} = \left( \frac{\rho_{wl} N_w}{\rho_{sch} L_{sch}} \right) \tau_{c,sch} e^{\frac{E_{sch}-E_{wl}}{K_B T}} \quad (13)$$

where  $L_{sch}$  is the total thickness of the SCH,  $\rho_{wl}$  is the Density of states per unit area in the WL and  $\rho_{sch}$  is the density of states per unit volume in SCH are given by [7],

$$\rho_{wl} = \frac{m_{ewl} K_B T}{\pi \hbar^2} \quad (14)$$

$$\rho_{sch} = 2 \left( \frac{2\pi m_{esch} K_B T}{\hbar^2} \right)^{\frac{3}{2}} \quad (15)$$

The photon lifetime is given by [8],

$$\frac{1}{\tau_p} = v_g (\alpha_{int} + \alpha_m) \quad (16)$$

where  $v_g = c/\mu_g$ ,  $\alpha_{int}$  is the internal loss,  $\alpha_m$  is the mirror losses.

$$S_{po} = \frac{n_{po}}{N_D} \quad (17)$$

where  $n_{po}$  is the number of photons in the cavity at steady state.

### 3-Output Optical Power

The output optical power emitted from the front facet of QD-LD is given by [9],

$$P_{out} = S_o \hbar\omega q \alpha_m v_g V \quad (18)$$

where  $S_o$  is the photon volume density at steady state,  $V$  is the cavity volume,  $\hbar\omega$  is the energy per photon,  $\hbar$  is a modification of Planck's constant is equal to  $h/2\pi$  and  $h$  is Planck's constant.

### 4-Gain and Efficiency

The optical gain of the GS of the QD laser diode is given by [8],

$$g_{GS} = G_{max}(2P_{GS0} - 1) \quad (19)$$

where  $P_{GS0}$  is occupation probabilities of GS of a QD at steady state and  $G_{max}$  is a maximum modal gain of the GS and the relation in reference [8] is used to calculate the  $G_{max}$ . At the threshold the current density must be high enough so that the gain can compensate the  $\alpha_i$  and  $\alpha_m$ , where the mirror loss given by [8],

$$\alpha_m = \frac{1}{2L} \ln \frac{1}{R_f R_b} \quad (20)$$

where  $R_f$  and  $R_b$  are the front and back reflectivities of the two mirror facets respectively.

A quantity of practical interest is the slope of the power-current curve for  $I > I_{th}$  it is called the slope efficiency is given by [10],

$$\frac{\Delta P_{out}}{\Delta I} = \frac{\hbar\omega}{2q} \eta_d \quad (21)$$

where, the quantity  $\eta_d$  is called the differential quantum efficiency, as it is a measure of the efficiency with which light output increases with an increase in the injected current given by [10],

$$\eta_d = 2 \frac{\Delta P_{out}}{\Delta I} \frac{\lambda}{1.24} \quad (22)$$

$$P_{in} = V_b I \quad (23)$$

where  $P_{in}$  is the input power,  $V_b$  is the bias voltage,  $\lambda$  is the wavelength.

### 5-Band Structure

The nanometer-sized InAs QDs represent localization centers for both electrons and holes since the bandgap of InAs is lower than that of the surrounding GaAs and InGaAs, therefore, the bandgap energy ( $E_g$ ) of InAs-QDs is about 0.354 eV,

embedded in wider bandgap wetting layers (InGaAs -WL) with  $E_g \approx 1.24$  eV, then a barrier layer of GaAs with  $E_g \approx 1.4$  eV then, cladding layers of AlGaAs with  $E_g \approx 2.2$  eV. The charge carriers build up and population inversion forms in the QD active layer due to carrier confinement, and as a result, enables lasing. The energy diagram of a proposed QD laser diode is shown in Figure (2). A wider bandgap semiconductor can have a lower refractive index, therefore AlGaAs has lower refractive index than that of GaAs, and the GaAs has lower refractive index than that of InAs QDs. The InAs QDs active region of higher refractive index is sandwiched between GaAs and AlGaAs cladding layer of lower refractive index to get a good confinement.

### 6-Structure Design of QD Laser Diode

The basic structure consists of an active region comprising QD layer embedded between two cladding layers. The bottom cladding is generally n-doped whereas the top cladding is p-doped. Then by cleaving the device, semiconductor/air interfaces are created to realize mirrors with approximately 30% reflectivity. Electrical confinement is provided by openings in the dielectric cover layer. The schematic illustration of the QD laser diode structure is shown in figure (3).

The dimensions of the proposed model of the InAs QD laser diode structure and the different layers are:

1. Bottom contact (Ni/AuGe/Au) 0.1  $\mu\text{m}$  layer thick, (is connected to the negative electrode of D.C supply) with stripe of 4  $\mu\text{m}$ .
2. n-GaAs substrates is grown. All samples (layers) were grown on it.
3. Afterwards a 300 nm thick n-GaAs buffer layer.
4. Afterwards a 50 nm thick of n-AlGaAs cladding layer
5. Active region length ( $L= 800 \mu\text{m}$ ), width ( $W_o= 12 \mu\text{m}$ ) and height ( $H_o= 375 \text{ nm}$ ), as shown in figure (4), with the following contents,

- a. Barrier layer thickness ( $L_{sch}$ ) as thin GaAs spacer in between the QD layers with thickness of 90 nm.
  - b. InGaAs wetting layer thickness ( $L_{wl}$ ) is 1 nm.
  - c. QD is disk shaped with height ( $L_d$ ) 2 nm and diameter ( $\rho$ ) 14 nm.
  - d. Number of QDs layers are five layers and the QDs surface density per layer is  $7 \times 10^{12} \text{ cm}^{-2}$ .
6. Afterwards a 50nm thick of p-AlGaAs cladding layer.
  7. p-GaAs cap layer 60nm thick.
  8. SiO<sub>2</sub> insulating layer is 0.1 $\mu\text{m}$  thick.
  9. Top contact of (Ti/Pt/Au) with thickness of 0.1  $\mu\text{m}$  is connected to the positive electrode of D.C supply.

The total width (W) is 100  $\mu\text{m}$  and length (L) is 800  $\mu\text{m}$  for the QD laser diode. The tables (1) and tables (2) are the material parameters and design parameters of the proposed QD laser diode respectively.

## 7-RESULTS

The main results of the QD laser diode operating characteristics can be summarized as follows:

- Power-current-voltage characteristics show that, the linear relation with small threshold current is 2.9 mA; threshold current density is 30.42 A/cm<sup>2</sup>, for the output optical power range (0-25 mW) and operating voltage is 0.954 V. The slope efficiency is 0.25 W/A, and high differential quantum efficiency is 80%, as shown in Figures (5), (6) and (7).
- Output optical power and input electrical power characteristics show that there is a linear relation with conversion efficiency of 71% as shown in Figure (8).
- Power spectra; optical output power of QD laser diode is emitted over the wavelength range of 1298-1305 nm which approaches 1.3  $\mu\text{m}$  wavelength

of optical fiber as shown in Figures (9) and (10).

- Photon and carrier population characteristics show that, when the carrier population reaches  $7 \times 10^6$ , the GS state begins emitting photons as shown in Figure (11) and (12).
- Gain characteristic show that, the optical gain increases to the threshold gain and then becomes fixed with increasing injection current. The optical gain of GS is saturated at maximum value of 44.6 cm<sup>-1</sup>, as shown in Figure (13).

## 8-CONCLUSIONS

The design successfully demonstrated the emission at room temperature under conditions of current injection at a wavelength of around under wavelength range (1298-1305 nm) from edge emitting laser diode structure. This indicates that it has long-wavelength and novel infrared light-emitting devices for optical fiber communications systems. Additionally, InAs-based QD on GaAs may become useful material for producing light emitters for QD-laser diode technology. A suitable choice of cavity dimensions yields devices which exhibit either an extremely low Room temperature threshold current of 2.93 mA, current density of 30.42 A/cm, an output power as high as 25 mW, ground state optical gain is 44.2 cm<sup>-1</sup>, slope efficiency is 0.25 W/A, and high differential quantum efficiency of 80%, with high conversion efficiency of 71% are obtained for a device with a better of characteristics suitable for optical fiber communications applications.

## 9-REFERENCES

- [1] E. O. Chukwuocha and M.C Onyeaju, "Simulation of Quantum Dots (QDs) in the Confinement Regime", *Ijaser Int., J. of Applied Sciences and Engineering Research*, Vol. 1, Issue 6, 2012.
- [2] I. Kaiander, "MOCVD Growth of InGaAs/GaAs QDs for Long Wavelength Lasers and VCSELs", Ph.D. thesis, Department of Mathematics and Natural Sciences, University of Berlin, 2006.
- [3] D. G. Nahri, H. Arabshahi and M. R. R. Abadi, "Analysis of Dynamic and Static Characteristics Of InGaAs/GaAs Self-Assembled Quantum Dot Lasers", *Armenian*,

J. of Physics, Vol. 3, No. 2, pp. 138-149, 2010.

[4] M. Gioannini, A. Sevega and I. Montrosset, "Simulations of Differential Gain and Linewidth Enhancement Factor of Quantum Dot Semiconductor Lasers", Springer, J. of Optical and Quantum Electronics 38, pp. 381–394, 2006.

[5] H. Al-Husseini, A. H. Al-Khursan and S. Y. Al-Dabagh, "III-Nitride QD Lasers", Journal of the Open Nanoscience, Vol. 3, pp. 1-11, 2009.

[6] A. Fiore and A. Markus, "Differential Gain and Gain Compression in Quantum-Dot Lasers", IEEE, Journal of Quantum Electronics, Vol. 43, No. 3, March 2007.

[7] M. Gioannini and I. Montrosset, "Numerical Analysis of the Frequency Chirp in Quantum-Dot Semiconductor Lasers", IEEE, J. of Quantum Electronics, Vol. 43, No. 10, October 2007.

[8] M. Ishida, N. Hatori, T. Akiyama, K. Otsubo, and Y. Nakata, "Photon Lifetime Dependence of Modulation Efficiency and K Factor in 1.3μm Self-Assembled InAs/GaAs Quantum-Dot Lasers: Impact of Capture Time and Maximum Modal Gain on Modulation Bandwidth", American Institute of Physics,

Applied Physics Letters, Vol. 85, No.18, 1 Nov. 2004.

[9] F. Grillot, B. Dagens, J. Provost, H. Su and L. F. Lester, "Gain Compression and above Threshold Linewidth Enhancement Factor in 1.3μm InAs–GaAs Quantum Dot Lasers", IEEE, J. of Quantum Electronics, Vol. 44, No. 10, Oct. 2008.

[10] Q. Cao, S. F. Yoon, C. Y. Liu and C. Y. Ngo, "Narrow Ridge Waveguide High Power Single Mode 1.3μm InAs/InGaAs Ten-Layer Quantum Dot Lasers", Nano Express, Nanoscale Res. Lett. 2, pp. 303-307, 2007.

[11] E. O. Chukwuocha and M.C Onyeaju, "Simulation of quantum dots (QDs) in the confinement regime", Ijaser Int., J. of Applied Sciences and Engineering Research, Vol. 1, Issue 6, 2012.

[12] J. Siegert, "Carrier Dynamics in Semiconductor Quantum Dots", Ph.D. thesis, Department of Microelectronics and Applied Physics, Royal Institute of Technology, 2006.

[13] Pierre Petroff's, "Quantum Dots and Quantum Rings Behave like Atoms", solid state research group at the University of California at Santa Barbara (UCSB), June 22, 2000.

Table (1) Material parameters of InAs-QD, InGaAs-WL and GaAs-SCH material system [4], [11] and [12]

Material parameters	Symbol	Value	Units
ES and GS recombination time	$\tau_r$	2.8	ns
SCH recombination time	$\tau_{sr}$	4.5	ns
WL recombination time	$\tau_{wr}$	3	ns
Capture time from WL to ES	$\tau_{c,wl}$	1	ps
Capture time from ES to GS	$\tau_{c,ES}$	7	ps
Diffusion time in SCH	$\tau_{c,sch}$	6	ps
Energy separation (SCH and WL) state	$E_{SCH-WL}$	84	meV
Average Energy separation (WL and ES) state	$E_{WL-ES}$	100	meV
Average Energy separation (ES and GS)	$E_{ES-GS}$	80	meV
Free electron mass	$m_o$	$9.11*10^{-31}$	Kg
InAs-QD electron effective mass	$m_e$	$0.065m_o$	Kg
InAs-QD heavy holes effective mass	$m_{hh}$	$0.377m_o$	Kg
InAs-QD refractive index	$\mu_{QD}$	3.52	-
GaAs-SCH refractive index	$\mu_{sch}$	3.65	-
InGaA- WL refractive index	$\mu_{wl}$	3.53	-
Degeneracies of GS and ES	$D_{GS}, D_{ES}$	2, 4	-

Table (2) Suggested design parameters.

Laser parameters	Symbol	Value	Units	Ref.
Active region width	$W$	12	$\mu\text{m}$	-
Active region length	$L$	800	$\mu\text{m}$	-
SCH thickness	$L_{sch}$	90	nm	-
WL thickness	$L_{wl}$	1	nm	-
Number of QD layers	$N_w$	5	-	-
QD surface density per layer	$N_d$	$7 \times 10^{12}$	$\text{cm}^{-2}$	-
Front mirror reflectivity	$R_f$	30%	-	-
Back mirror reflectivity	$R_b$	90%	-	-
Internal loss	$\alpha_{int}$	1	$\text{cm}^{-1}$	[4]
Spontaneous emission factor	$\beta$	$10^{-4}$	-	[4]

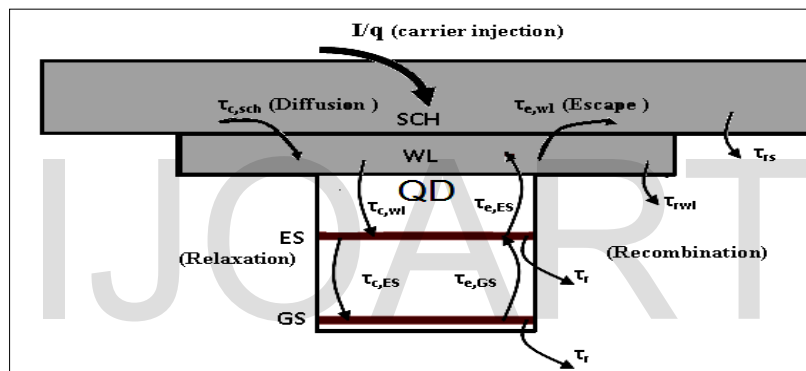


Figure (1) Schematic diagram of the components in InAs-QD, InGaAs-WL and GaAs-SCH material system [4]

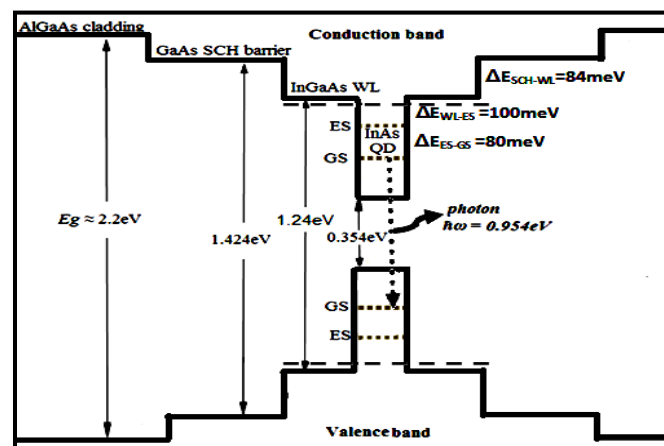


Figure (2) Energy difference diagram in the CB and VB for QD laser diode

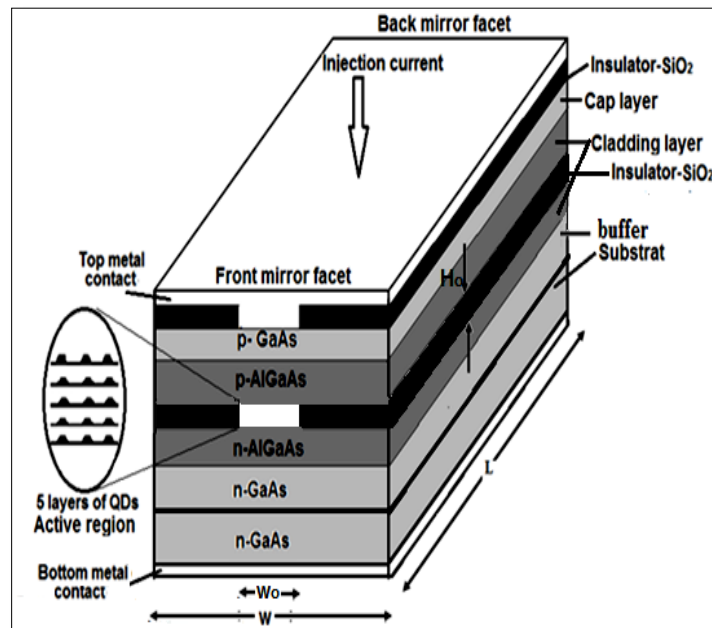


Figure (3) Schematic illustration of QD laser diode structure

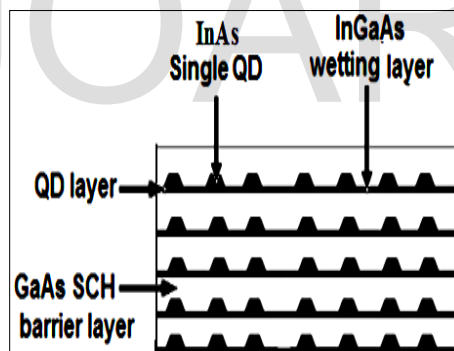


Figure (4) Schematic diagram of the active region cross-sectional view for QD laser diode



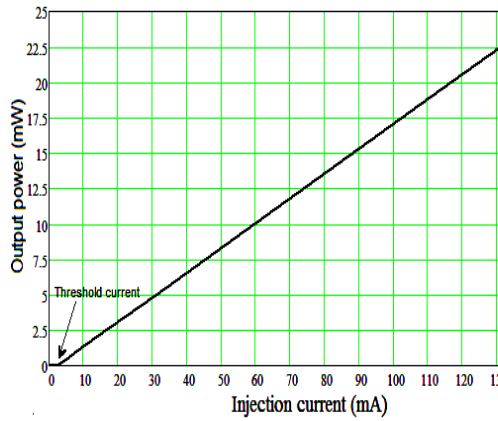


Figure (5) Power vs. current characteristics

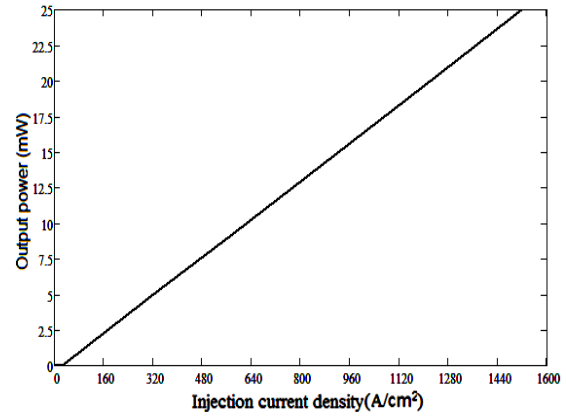


Figure (6) power vs. current density characteristics

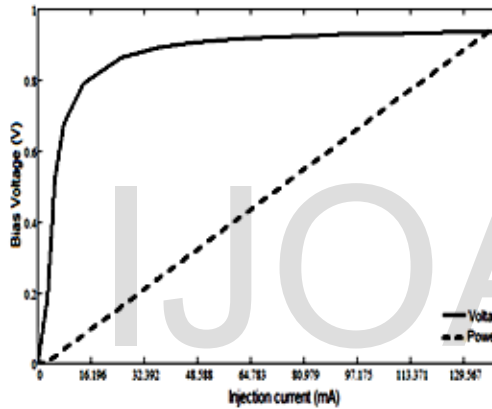


Figure (7) Voltage, current and output power characteristics

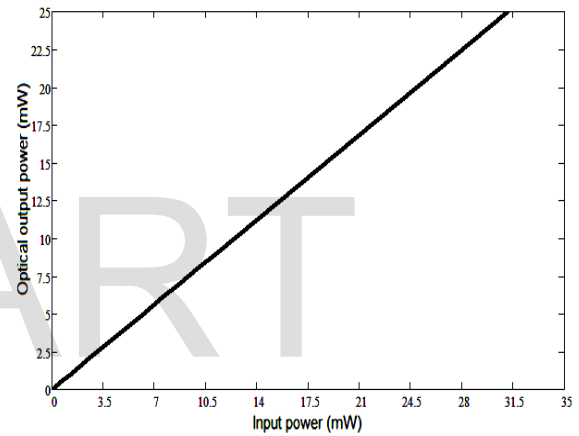


Figure (8) Input power and output characteristic

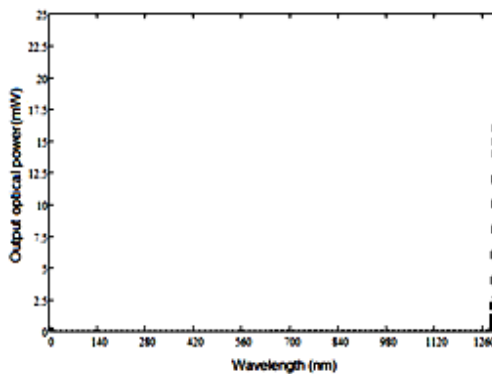


Figure (9) Power spectra

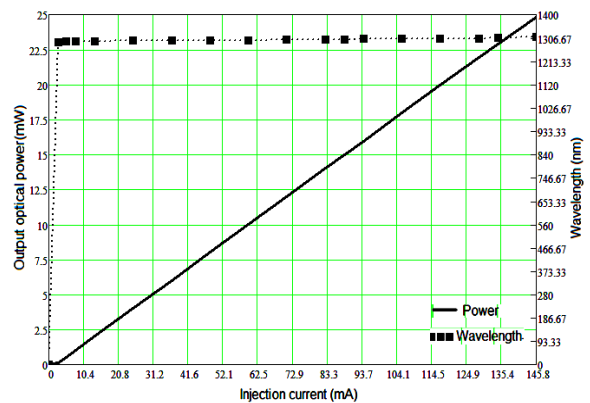


Figure (10) Output power and emitting wavelength with respect to the current

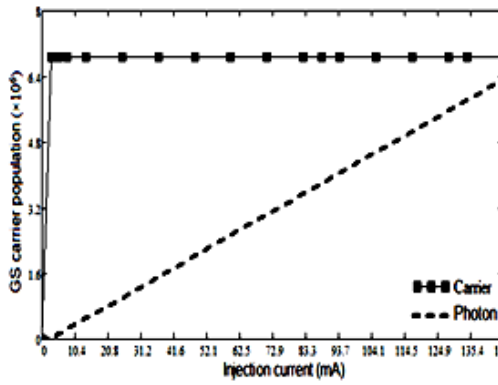


Figure (11) Carrier population of GS as a function of injection current

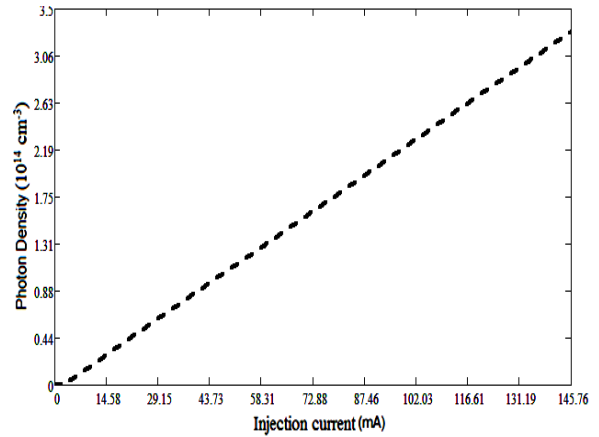


Figure (12) Photon density as a function of injection current

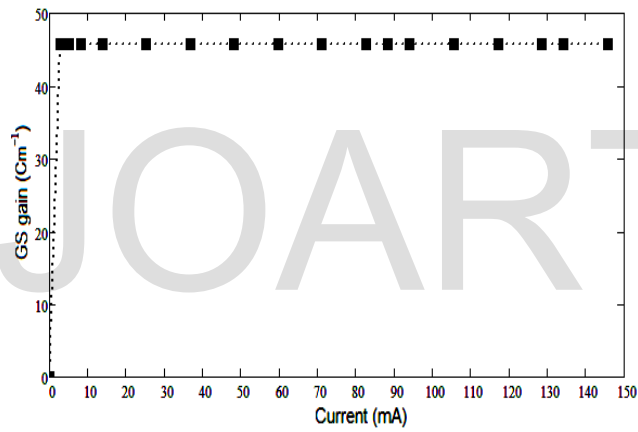


Figure (13) optical GS laser gain as a function of injection current